JOURNAL OF OPTOELECTRONICS AND ADVANCED MATERIALS, Vol. 11, No. 11, November 2009, p. 1773 - 1778

Optical and infrared properties of a series of pyramidalized olefin Pt-complexes - DFT study

C. I. OPREA[a], F. MOSCALU[a], A. DUMBRAVĂ[b], S. IOANNOU[c], A. NICOLAIDES[c], M. A. GÎRȚU[a]
[a]*Department of Physics, Ovidius University of Constanța, Bd. Mamaia 124, 900527 Constanța, România*
[b]*Department of Chemistry, Ovidius University of Constanța, Bd. Mamaia 124, 900527 Constanța, România*
[c]*Department of Chemistry, University of Cyprus, Nicosia 1678, Cyprus*

We report Density Functional Theory (DFT) calculations providing the geometrical and electronic structures, as well as the vibrational and optical properties of the homologous series of Pt-pyramidalized olefin complexes $(CH_2)_n$-$(C_8H_{10})Pt(PX_3)_2$, where X = H and Ph, and n = 0, 1, 2, and 3. All complexes were geometry optimized for the singlet ground state in vacuum using DFT methods with B3LYP exchange-correlation functional and the Effective Core Potential LANL2DZ basis set, within the frame of Gaussian03 quantum chemistry package. Electronic transitions were calculated at the same level of theory by means of Time Dependant-DFT. For both X = H and X = Ph complexes and regardless of n, the electronic absorption bands are located in the UV region of the spectrum, most transitions being assigned to metal to ligand charge transfers. We compare and contrast the complexes revealing the role of the number of CH_2 groups, n, on the geometry, and infrared and optical spectra. The relevance of these Pt-based compounds as possible pigments for dye-sensitized solar cells is discussed.

(Received November 4, 2009; accepted November 12, 2009)

Keywords: Density functional theory, Electronic structure, Infrared and optical spectra, Olefin, Dye-sensitized solar cells

1. Introduction

Platinum-olefin complexes have a rich history as ligands in organometallic chemistry, being of great importance in the field of asymmetric catalysis [1]. The lability of olefin ligands ensures rapid and quantitative exchange reactions, which allows in situ preparation of optically active catalyst systems. Several such Pt-olefin complexes were found to display a pyramidalized structure [2]. Pyramidalized alkenes are molecules containing carbon–carbon double bonds in which one or both of the sp^2 carbon atoms do(es) not lie in the same plane as the attached atoms [2,3]. Alkenes of this kind are also interesting due to their intriguing physical properties and their fascinating reactivity [4].

Ab initio and density functional theory (DFT) calculations have been applied to several highly pyramidalized alkenes in order to understand and explain their structures, properties and reactivities [5,6,7]. Quantum-chemical calculations of simple model complexes with specified pyramidalization angles revealed a significant strengthening of the metal–alkene bond relative to that in complexes of the planar alkenes [8].

In the homologous series of $(CH_2)_n$-$(C_8H_{10})Pt(PX_3)_2$, (n = 0, 1, 2, and 3, and X = H, Ph) pyramidalized olefins the energy of the LUMO depends strongly on n, the number of the methylene groups of the bridge [8,9,10]. Thus, the electron accepting ability of the olefin is changed by going from n = 3 to n = 0, and this affects in a systematic way the charge transfer from the ligands to the Pt and to the olefin. Therefore, the number, n, of the methylene groups of the bridge provides a handle for systematic fine-tuning of the optical properties of these systems, which triggered the interest to explore the possibilities of using such systems in dye-sensitized solar cells (DSSC) [11].

Dye-sensitized solar cells are devices for the conversion of visible light into electricity based on sensitizing a wide bandgap semiconductor, such as nanocrystalline anatase TiO_2, with a dye (for instance ruthenium(II) polypyridyl complexes with carboxylated ligands), presenting intense visible metal-to-ligand charge transfer bands [12]. The search for new dyes, either based on metallorganic complexes [13] or organic molecules [14,15] has stimulated theoretical calculations, DFT methods being applied to large molecules with reasonable accuracies, allowing for the description of the absorption spectrum of the dye [16,17]. The bonding of the dye to the nanoparticle, the alignment of the energy levels of the two subsystems, the transfer of the electron from the dye to the cluster have all been successfully calculated by means of a DFT approach [16] .

We report here an investigation of the $(CH_2)_n$-$(C_8H_{10})Pt(PX_3)_2$ complexes by DFT calculations of the structural and electronic properties, as well as of the IR and UV-Vis spectra. We study the role of the number of the methylene groups of the bridge on the geometry and optical properties of these complexes and discuss on the possibility to use them in DSSCs.

2. Computational details

The geometrical structures of the $(CH_2)_n$-$(C_8H_{10})Pt(PX_3)_2$, X = H and Ph, n = 0, 1, 2, and 3 complexes were optimized using the Density Functional Theory with the hybrid B3LYP exchange-correlation

functional [18]. The Los Alamos Effective Core Potential (ECP) [19] and double-ζ quality functions for valence electrons [20] were used by employing the LANL2DZ basis set. Optical absorption spectra of all complexes, including the lowest 40 singlet-singlet excitations, were simulated using the Time Dependent -DFT (TD-DFT) method. All calculations were performed with the GAUSSIAN03 package [21].

3. Results and discussion

The geometrical structures were optimized for the singlet ground state of all complexes. The symmetry group of the neutral X = H complexes is C_{2v} for $n = 0$ and $n = 1$, C_2 for $n = 2$, and C_1 for $n = 3$. Figure 1 displays the structure of the X = H complexes for all values of n. Bond lengths and angles between atoms coordinated to Pt ion are given in Table 1, along with parameters from previous studies, both theoretical, performing similar DFT/B3LYP calculations [10,22] and experimental, providing the X-ray structure of related complexes, with the phosphine hydrogens replaced by phenyl rings [23]. The results in Refs. [10,22] were obtained using polarization functions on all heavy atoms at the expense of computational time (ECP and D95** basis set in Ref. [10] and G2 basis set in Ref. [22]), whereas in our calculations no *d*-functions were used on phosphorus atoms in order to speed-up calculations. We note a good agreement between our and previous calculations for the Pt-C and C=C bond lengths computed without and with polarization functions, respectively, the differences being less than 0.03 Å. We also note the increase in the Pt-C bond length and the decrease of the C=C bond length upon increasing n. The agreement between methods on Pt-P bond lengths is satisfactory, as not considering the *d*-functions on P atoms gives bonds longer by 0.07 Å (2.42 Å as compared to 2.35 Å in Ref. [10]). However, the close agreement between our calculated and the observed Pt-C and C=C bond lengths indicates that the deficiency in the basis set has negligible effect on the description of the metal-olefin bonding. For the n = 2 and 3 complexes the four atoms coordinating to Pt are not coplanar, the dihedral angle being 3.1° and 0.6°.

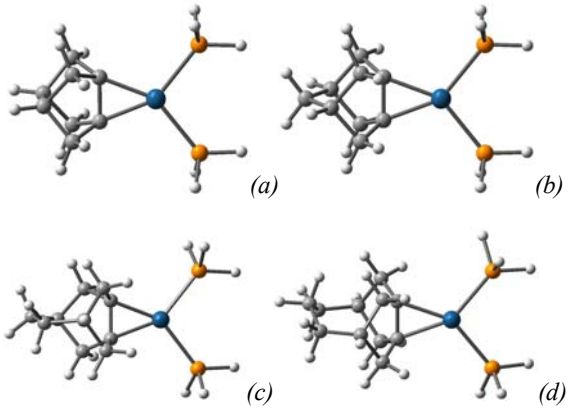

Fig. 1 Optimized structures of the n = 0 (a), n = 1 (b), n = 2 (c), n = 3 (d), for $(CH_2)_n$-$(C_8H_{10})Pt(PH_3)_2$ complexes.

Table 1. Optimized parameters of the first coordination sphere of the Pt ion in neutral $(CH_2)_n$-$(C_8H_{10})Pt(PX_3)_2$ complexes compared with calculated parameters from Ref. [10,22] and experimental values from Ref. [23]. Bond lengths are given in Å, bond angles and dihedral angles in deg.

	X = H									**X = Ph**				
Parameter	$n = 0$			$n = 1$		$n = 2$		$n = 3$		$n = 0$	$n = 1$		$n = 2$	$n = 3$
		Ref. 22	Ref. 10		Ref. 10		Ref. 10		Ref. 10			Ref. 23		
r(Pt-C)	2.09	2.10	2.10	2.11	2.12	2.12	2.13	2.14	2.15	2.10	2.11	2.07	2.13	2.14
r(Pt-P)	2.42	2.35	2.33	2.43	2.32	2.43	2.32	2.43	2.32	2.46	2.46	2.30	2.46	2.47
r(C=C)	1.54	1.51	1.51	1.50	1.48	1.48	1.46	1.47	1.45	1.54	1.50	1.48	1.48	1.47
θ(P-Pt-P)	103.6	106.0	105.6	103.9	106.4	103.1	106.6	102.9	106.5	108.0	101.8	-	101.9	102.2
θ(C=C-Pt-P)	0.0	0.0	0.0	0.0	0.0	3.1	2.8	0.6	0.9	7.2	6.1	-	7.8	6.2
ϕ(C-C-C=C)	72.1	71.9	71.9	65.1	64.9	58.7	58.4	53.0	52.2	72.3	65.5	60	59.3	53.8

The degree of pyramidalization can be measured using the pyramidalization angle (ϕ) as defined by Borden and coworkers [2,9], between the plane containing one of the doubly bonded carbon atoms and the two substituents attached to it and the extension of the double bond. Although strictly speaking, the ϕ angle is applicable only to those cases involving C_{2v} symmetry, we note that the ϕ angle decreases with increasing n, for both X = H and X = Ph systems. Regardless of X, ϕ decreases with almost 20°, from ~72° for $n = 0$ to ~53.0° for $n = 3$, in steps of about 6°. Moreover, the comparison of our results with other studies using *d*-functions in the basis sets [10,22] shows that the absence of such functions for the P atoms does not have a significant influence on the pyramidalization angle.

Table 1 also displays structural data for X = Ph. The symmetry group of the neutral X = Ph complexes is C_2 for $n = 0$, $n = 1$, and $n = 2$, and C_1 for $n = 3$. The comparison with the experimental results of Ref. [23] indicates some

deviations especially in the case of the Pt-P distance and in the pyramidalization angle, the calculated results overestimating the experimental values.

The analysis of vibration modes reveals for the $(CH_2)_n$-$(C_8H_{10})Pt(PH_3)_2$ complexes three main peaks, regardless of n (see Fig. 2). For $n = 0$ we find three intense peaks in the IR spectrum at frequencies of 1004.4 cm^{-1}, 2283.4 cm^{-1}, and 3113.3 cm^{-1}. These peaks are assigned to asymmetric umbrella-like vibrations of phosphine hydrogens, symmetric stretch of one hydrogen atom per phosphine, along the symmetry axis, and asymmetric vibrations of methylene hydrogen atoms, respectively. As expected, the increase in the number of methylene groups affects mostly the high energy peak, leading to a reduction of the vibration frequency.

Except for the middle peak, the values of the vibration frequencies for $n = 0$ compare reasonably to the results obtained with larger basis sets (1008.2 cm^{-1}, 2394.2 cm^{-1}, and 3089.1 cm^{-1}, respectively, according to Ref. [10]).

For the $(CH_2)_n$-$(C_8H_{10})Pt(PPh_3)_2$ complexes the IR spectrum is more complex, as it includes features of the phenyl rings (Fig. 2). For $n = 0$ the highest intensity peaks are at high frequencies, at 3109.9 cm^{-1} and 3227.8 cm^{-1}. At 3227.8 cm^{-1} we find a C-H bond stretching in the phenyl rings along the symmetry axis (roughly perpendicular on the plane formed by Pt and C=C atoms), whereas at 3109.9 cm^{-1} we get vibrations of the hydrogen atoms on the methylene groups and olefin. At 1512.8 cm^{-1} the vibration is a in plane "rocking" of the two phenyl rings roughly parallel with the Pt-C=C plane, whereas at 1043.2 cm^{-1} it is an out-of-plane "rotation" of the hydrogen atoms of the phenyl rings perpendicular on the Pt-C=C plane. Two close peaks are located at 725.4 cm^{-1} and at 782.0 cm^{-1} representing an out-of-plane "rotation" for the hydrogen atoms of all phenyl rings and an out-of-plane "rotation" of the hydrogen atoms of the phenyl rings parallel with the Pt-C=C plane, respectively. At lower frequencies, at 530.0 cm^{-1} the vibration mode is an out-of-plane "rotation" for the hydrogen atoms of all phenyl rings similar to the peak at 725.4 cm^{-1}.

Overall the IR spectra of the $(CH_2)_n$-$(C_8H_{10})Pt(PPh_3)_2$ complexes are qualitatively similar. We observe that the increase of n affects to a larger extent the peak at 3109.9 cm^{-1}, as expected, as it involves the hydrogen atoms on the olefin.

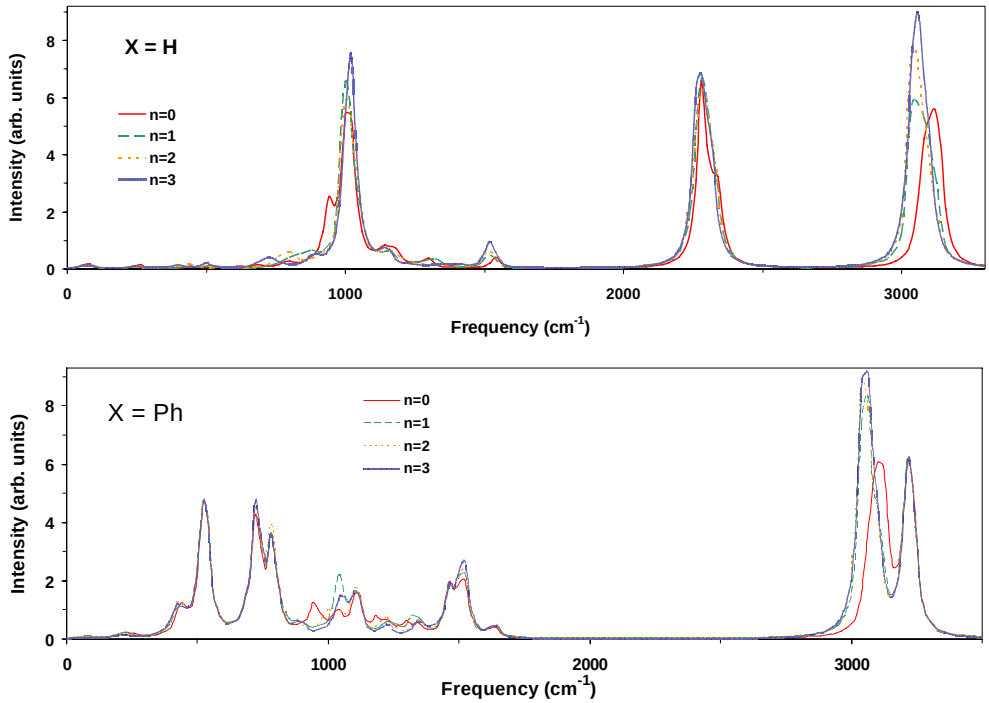

Fig. 2 Calculated IR absorption spectra of $(CH_2)_n$-$(C_8H_{10})Pt(PX_3)_2$ complexes for n = 0, 1, 2 and 3, with X = H (top) and X = Ph (bottom).

For all $(CH_2)_n$-$(C_8H_{10})Pt(PX_3)_2$ complexes (n = 0, 1, 2 and 3, X = H and X = Ph), the UV-Vis absorption spectra, calculated by TD-DFT, are displayed in Fig. 3.

We note that in all cases the absorption bands are in the near UV range. In each case, the lowest band corresponds to a HOMO → LUMO transition. For X = H, taking as reference the $n = 0$ complex, we find transitions at 4.27 eV (associated with a HOMO → LUMO transition), 4.64 eV (HOMO → LUMO+2), 4.98 eV (HOMO-2 → LUMO), and 5.64 eV (HOMO-2 → LUMO+1). For $n = 1$, 2 and 3 the spectra are qualitatively similar, but red-shifted. The shifts can be examined in Table 2, which presents the energy values of the most intense transitions in each band of the UV-Vis spectra shown in Fig. 2. The decrease in energy when increasing n is, for the most intense peaks, 0.24 eV

between 0 and 1, 0.11 eV between 1 and 2, and 0.13 eV between 2 and 3.

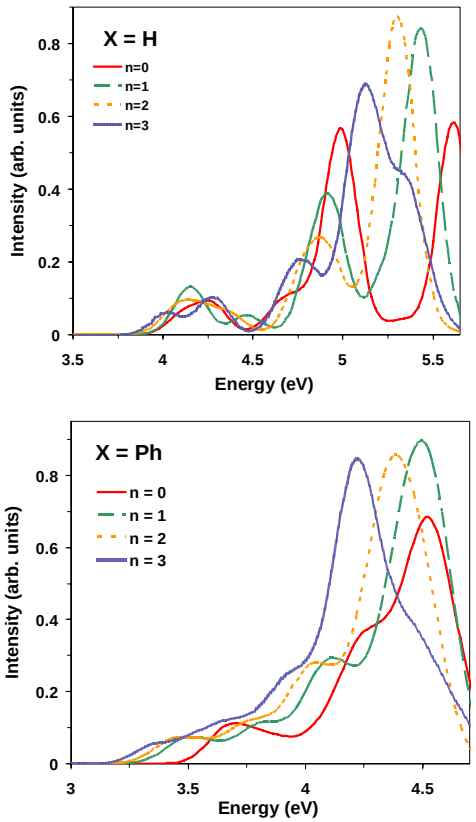

Fig. 3 Calculated UV-Vis absorption spectra of of $(CH_2)_n$-$(C_8H_{10})Pt(PX_3)_2$ complexes for n = 0, 1, 2 and 3, with X = H (left) and X = Ph (right).

We also note the variation in intensity caused by the change in the number of CH_2 groups. For instance, the highest peak in the spectrum has an increase in intensity from $n = 0$ to $n = 1$, as well as from 1 to 2, which correlates with a decrease in intensity for the lower energy peaks. From $n = 2$ to $n = 3$ the highest intensity peak looses some of the intensity as the band broadens, with a shoulder at 5.37 eV.

Table 2. Energy (in eV) of the most intense transitions in each band for $(CH_2)_n$-$(C_8H_{10})Pt(PX_3)_2$ complexes.

X = H				X = Ph			
n = 0	n = 1	n = 2	n = 3	n = 0	n = 1	n = 2	n = 3
4.27	4.13	4.07	4.02	3.66	3.47	3.43	3.35
4.64	4.47	4.38	4.26	4.07	3.78	3.73	3.65
4.98	4.94	4.90	4.78	4.22	4.07	4.05	4.04
5.64	5.40	5.29	5.16	4.54	4.47	4.35	4.22

In the case of the X = Ph complexes the transitions are more closely spaced, with the lowest 40 transitions below 4.7 eV. Similar to the previous case, the increase of n leads to a shift of the spectrum towards lower energies, as it can be seen from Table 2. The decrease in energy when increasing n is, for the most intense peaks, 0.07 eV between 0 and 1, 0.12 eV between 1 and 2, and 0.13 eV between 2 and 3.

The variation in the intensity of the highest intensity peak caused by the change in the number of CH_2 groups is inversely correlated with the variation in intensity of the adjacent lower energy peak.

To better understand the nature of the transitions we looked at the electron density of the HOMO and LUMO, the most relevant molecular orbitals for $(CH_2)_n$-$(C_8H_{10})Pt(PH_3)_2$, shown in Fig. 4. Regardless of n, the HOMO is localized on the d_{z2} orbitals of the metal and the π bond of the olefin, whereas the LUMO is mainly localized on the phosphine ligands.

Fig. 5 displays the electron density for the molecular orbitals of (CH_2)-$(C_8H_{10})Pt(PH_3)_2$ with the most important contribution in the most intense transitions. In this case, of $n = 1$, the HOMO-2 is localized in a d_{x2-y2} orbital displaying a σ bond with the carbon atoms of the olefin. The LUMO+1 is shared by phosphine hydrogen atoms, the d_{x2-y2} of the Pt and the π^* of the olefin; in this case we see a σ^* antibonding orbital. LUMO+2 has high electron density mainly on the phosphorus atom, whereas LUMO+3 is localized on d_{x2-y2} orbitals of Pt and on P.

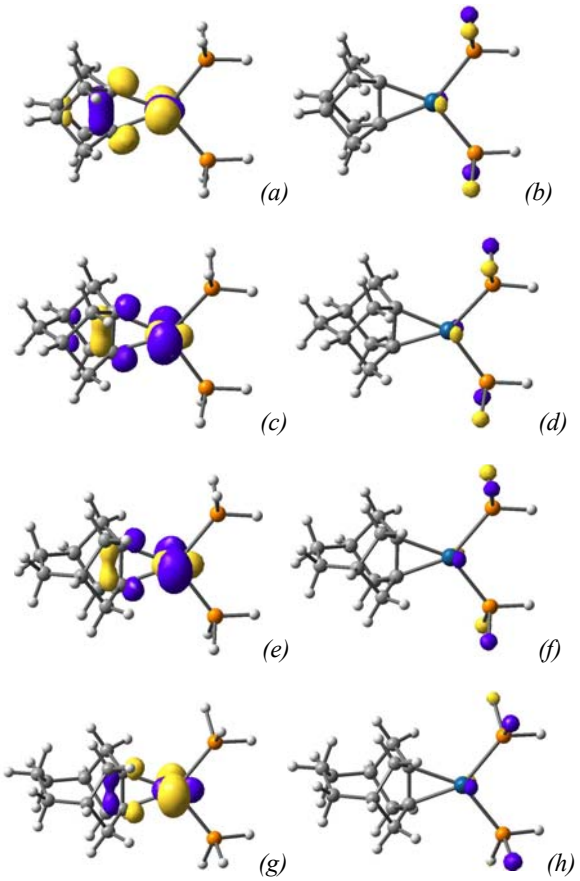

Fig. 4 Isodensity surfaces (0.075 e/bohr^3) of molecular orbitals of the $(CH_2)_n$-$(C_8H_{10})Pt(PH_3)_2$ complexes for: (a) HOMO and (b) LUMO of n = 0, (c) HOMO and (d) LUMO of n = 1, (e) HOMO and (f) LUMO of n = 2 and (g) HOMO and (h) LUMO of n = 3.

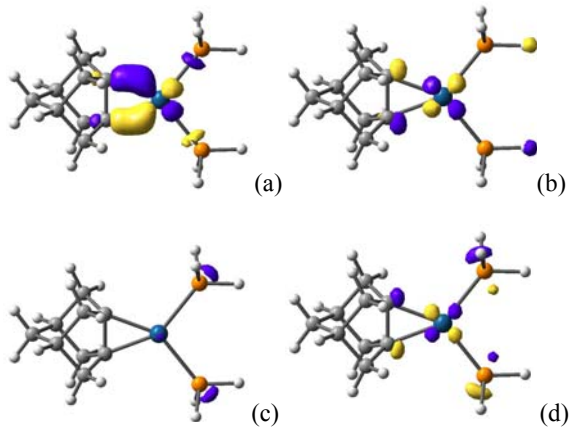

Fig. 5 Isodensity surfaces (0.075 e/bohr^3) of molecular orbitals of the (CH_2)-$(C_8H_{10})Pt(PH_3)_2$ complex: (a)HOMO-2 (48MO), (b) LUMO+1 (52MO), (c) LUMO+2 (53MO), (c) LUMO+3 (54MO).

The analysis of the composition of the main lines in each band is performed in Table 3. The lowest band, at 4.13 eV, =corresponds to a HOMO → LUMO transition.

Table 3. Energy, oscillator strength and composition of the most intense optical transitions in each band for the (CH_2)-$(C_8H_{10})Pt(PH_3)_2$ complex.

E(eV)	*f*	Composition	Obs.
4.13	0.014	0.686[50(a_1)→51(b_1)]	M→L
4.47	0.011	0.690[50(a_1)→53(a_1)]	M→L
4.94	0.026	-0.123[45(a_1)→52(b_2)] -0.214[47(a_2)→51(b_1)] +0.389[49(a_1)→52(b_2)] +0.279[50(a_1)→52(b_2)] +0.403[50(a_1)→54(b_2)] -0.120[50(a_1)→55(b_2)]	M→L
5.40	0.089	-0.370[45(a_1)→53(a_1)] +0.542[48(b_2)→52(b_2)] -0.120[49(a_1)→53(a_1)] +0.125[50(a_1)→57(a_1)]	M→L

Given that the HOMO is localized on the d_{z2} orbitals of the metal and the π bond of the olefin, whereas the LUMO is mainly localized on the hydrogen atoms of the phosphine group, the transition is a metal to ligand charge transfer. At 4.47 eV, we find a HOMO → LUMO+2 transition, from the metal to the phosphine ligand. At 4.94 eV the transition is more complex, the highest contribution coming from HOMO → LUMO+3, suggesting charge transfer from the olefin to the P atoms. The highest band, around 5.40 eV, is dominated by the HOMO-2 → LUMO+1 transition, which transfers the charge from the olefin to the hydrogen atoms of the phosphine group. Thus, for $(CH_2)_n$-$(C_8H_{10})Pt(PH_3)_2$ complexes, particularly for n = 1, all transitions are associated, to a large extent, to metal to ligand charge transfers. We note that we observed similar results for n = 2 [24] as well as for the X = Ph complexes [25].

Based on the absence of strong absorption bands in the visible region of the UV-Vis spectrum and considering the bandgap of the usual semiconductor used in DSSCs (~3.2 eV for TiO_2 [16]) it is unlikely that a system consisting of the $(CH_2)_n$-$(C_8H_{10})Pt(PX_3)_2$ complexes and the TiO_2 anatase nanoparticle can lead to a competitive efficiency of a DSSC.

4. Conclusions

We reported DFT calculations of the optimized geometry and electronic structure, as well as the vibrational and optical properties of Pt-pyramidalized olefin complexes: $(CH_2)_n$-$(C_8H_{10})Pt(PX_3)_2$, with X = H and Ph, and n = 0, 1, 2, and 3. The number, n, of CH_2 groups influences mostly the high frequency band in the infrared spectra, which is assigned to the asymmetric vibrations of methylene hydrogen atoms. We found, as expected, that the larger the n the smaller the vibration frequency of the complex.

A common feature in the electronic structure of all complexes, regardless of n, is the localization of the HOMO electron density on the platinum d_{z2} orbitals and the π bond of the olefin. Also, for all values of n, the LUMO is mainly localized on the phosphine ligands.

The optical spectra are strongly influenced by n, the methylene groups causing a systematic red-shift and strong variations in intensity. Careful analyses of the composition of the absorption UV-Vis transitions, demonstrated here in detail for n = 1, revealed the metal to ligand charge transfer character for all bands.

The relevance of these Pt-based compounds as possible pigments for dye-sensitized solar cells was discussed. Although the X = Ph complexes have lower energy electronic transitions than the X = H complexes, the absence of strong absorption bands in the visible region of the spectrum is unlikely to lead to a competitive efficiency when used in a TiO_2 based DSSC.

Acknowledgments

Funded by ANCS, the Romanian Authority for Scientific Research, grant PN2-Capacitati-M3 128/2009 and by the Research Promotion Foundation (RPF) of Cyprus (KY-POY/0407/04).

References

[1] C. Defieber, H. Grutzmacher, E.M. Carreira, Angew. Chem. Int. Ed. **47**, 4482 (2008).
[2] W. T. Borden, Chem. Rev. **89**, 1095 (1989); W. T. Borden, Synlett 711 (1996).
[3] S. Vázquez, P. Camps, Tetrahedron **61**, 5147 (2005).
[4] D. Margetic´, Y. Murata, K. Komatsu, M. Eckert-Maksic, Organometallics **25**, 111 (2006).
[5] M. C. Holthausen, W. Koch, J. Phys. Chem. **97**, 10021 (1993).

[6] S. Vázquez, J. Chem. Soc. Perkin Trans. **2**, 2100 (2002).
[7] G. Rasul, G. A. Olah, G. K. S. Prakash, J. Phys. Chem. A **110**, 7197 (2006).
[8] A. Nicolaides, J. M. Smith, A. Kumar, D. M. Barnhart, W. Thatcher Borden, Organometallics **14**, 3475 (1995).
[9] K. Morokuma, W.T. Borden, J. Am. Chem. Soc. **113**, 1912 (1991).
[10] F. A. Theophanous, A. J. Tasiopoulos, A. Nicolaides, X. Zhou, W. T. G. Johnson, W. Thatcher Borden, Org. Lett., **8**, 3001 (2006).
[11] M. Gratzel, Nature **414**, 338 (2001); M. Gratzel, J. Photochem. Photobiology A: Chem. **164**, 3 (2004).
[12] L. M. Peter, Phys. Chem. Chem. Phys. **9**, 2630 (2007).
[13] B. E. Hardin, E. T. Hoke, P. B. Armstrong, J.-H. Yum, P. Comte, T. Torres, J.M.J. Frechet, M. K. Nazeeruddin, M. Gratzel, M.D. McGehee, Nature Photonics **3**, 406, (2009).
[14] D. Kuang, S. Uchida, R. Humphry-Baker, S. M. Zakeeruddin, M. Gratzel, Angew. Chem. Int. Ed. **47**, 1923 (2008).
[15] A. Dumbravă, A. Georgescu, G. Damache, C. Badea, I. Enache, C. Oprea, M.A. Gîrţu, J. Optoelectron. Adv. Mater. **10**, 2996 (2008); A. Georgescu, G. Damache, M. A. Gîrţu, J. Optoelectron. Adv. Mater. **10**, 3003 (2008).
[16] F. De Angelis, S. Fantacci, A. Sgamellotti, Theor. Chem. Acc. **117**, 1093 (2007); F. De Angelis, S. Fantacci, A. Selloni, Nanotechnology. **19**, 424002 (2008).
[17] B. F. Minaev, V. A. Minaeva, G. V. Baryshnikov, M. A. Gîrţu, H. Ågren, Russian J. of Appl. Chem. **82**, 1211 (2009); B. F. Minaev, V. A. Minaeva, G. V. Baryshnikov, M. A. Gîrţu, H. Ågren, Journal of Experimental Nanoscience, in press.
[18] S. H. Vosko, L. Wilk, M. Nusair, Can. J. Phys. **58**, 1200 (1980); A. D. Becke, Phys. Rev. A**38**, 3098 (1988); J. P. Perdew, Y. Wang, Phys. Rev B **45**(13), 244 (1992).
[19] P. J. Hay, W. R. Wadt, J. Chem. Phys. **82**, 299 (1985);
[20] T. H. Dunning Jr. and P.J. Hay, In Modern Theoretical Chemistry; H.F. Schaefer III, Ed.; Plenum: New York, 1976; Vol. 3
[21] Gaussian 03, Revision C.02, M. J. Frisch, G. W. Trucks, H. B. Schlegel, G. E. Scuseria, M. A. Robb, J. R. Cheeseman, J. A. Montgomery, Jr., T. Vreven, K. N. Kudin, J. C. Burant, J. M. Millam, S. S. Iyengar, J. Tomasi, V. Barone, B. Mennucci, M. Cossi, G. Scalmani, N. Rega, G. A. Petersson, H. Nakatsuji, M. Hada, M. Ehara, K. Toyota, R. Fukuda, J. Hasegawa, M. Ishida, T. Nakajima, Y. Honda, O. Kitao, H. Nakai, M. Klene, X. Li, J. E. Knox, H. P. Hratchian, J. B. Cross, V. Bakken, C. Adamo, J. Jaramillo, R. Gomperts, R. E. Stratmann, O. Yazyev, A. J. Austin, R. Cammi, C. Pomelli, J. W. Ochterski, P. Y. Ayala, K. Morokuma, G. A. Voth, P. Salvador, J. J. Dannenberg, V. G. Zakrzewski, S. Dapprich, A. D. Daniels, M. C. Strain, O. Farkas, D. K. Malick, A. D. Rabuck, K. Raghavachari, J. B. Foresman, J. V. Ortiz, Q. Cui, A. G. Baboul, S. Clifford, J. Cioslowski, B. B. Stefanov, G. Liu, A. Liashenko, P. Piskorz, I. Komaromi, R. L. Martin, D. J. Fox, T. Keith, M. A. Al-Laham, C. Y. Peng, A. Nanayakkara, M. Challacombe, P. M. W. Gill, B. Johnson, W. Chen, M. W. Wong, C. Gonzalez, J. A. Pople, Gaussian, Inc., Wallingford CT, 2004.
[22] J. Uddin, S. Dapprich, G. Frenking, B. F. Yates, Organometallics, **18**, 457 (1998)
[23] A. Kumar, J.D. Lichtenthan, S.C. Critchlow, B. E. Eichinger, W.T. Borden, J. Am. Chem. Soc. **112**, 5633 (1990).
[24] C. I. Oprea, A. Dumbravă, F. Moscalu, A. Nicolaides, M. A. Gîrţu, AIP conference proceedings (BPU7 2009) in press.
[25] C. I. Oprea, F. Moscalu, A. Dumbravă, A. Nicolaides, M. A. Gîrţu, Rom. J. Phys. Submitted

*Corresponding author: girtu@univ-ovidius.ro